Multi-input Step-Up Converters Based on the Switched-Diode-Capacitor Voltage Accumulator

Shiying Hou, Jianfei Chen, Tao Sun, and Xiaohui Bi

***Abstract*—This paper introduces the application of a switched-diode-capacitor voltage accumulator (SDCVA) on conventional boost converter. This study aims to obtain two different kinds of multi-input step-up converters with high voltage gains, low component stresses, low ripples, simple control, and high conversion efficiencies: one is based on the parallel SDCVA and the other based on the serial SDCVA. The double-input step-up converter based on the parallel SDCVA and the double-input step-up converter based on the serial SDCVA are, respectively, taken as an example to do theoretical analysis, including operating principles and performance analyses when they work individually and simultaneously. The two proposed converters are implemented with a voltage closed-loop control at the switching frequency of 30 kHz. Experimental results obtained from the implemented prototypes are provided to validate the feasibility and effectiveness of the proposed converters.**

***Index Terms*—High efficiency, high voltage gain, low component stress, multi-input, simple control, switched-diode-capacitor voltage accumulator (SDCVA).**

I. Introduction

ENERGY sources such as photovoltaic cells (PVs), fuel cells (FCs), batteries, etc., play a very important role in distributed generation systems. The interconnection of the renewable and alternative energy sources is achieved through electronic interfaces. Therefore, power electronic interfaces become essential for the integration of different power generation units with distinct electrical characteristics into a common system while still achieving high efficiency and good performances [1].

To attain the goal of integration, a multi-input converter (MIC) is a perfect choice, which may integrate diverse power sources and provide power to a common load in a single conversion stage. Many papers related to a variety of MIC topologies have been published. In [2], a systematic approach to synthesizing MICs by introducing the pulsating voltage source cells and the pulsating current source cells into six basic PWM converters is proposed. Four rules that must be observed in order to be able to realize a MIC from its single-input version are listed in [3]. In the renewable power generation system, MIC topologies are usually integrated with a dc link. However, most of these MICs do not take high voltage gain into consideration, since the output of PVs, FCs, and batteries is typically unregulated low-level dc voltages that needs to be stepped up to regulated, high-level voltages for practical applications.

At present, the conventional boost converter is usually used because of its simple circuit. Unfortunately, practical considerations limit its output voltage to approximately four times its input voltage [4]. To supply a high output voltage, it must operate at extremely high duty-cycle whereas extreme duty-cycles impose inefficient small off times or low switching frequencies. Small off times will cause severe diode reverse-recovery currents, increasing electromagnetic interference (EMI) levels. And low switching frequencies may cause higher ripple currents and increase size of magnetic components. Significant switch and diode reverse-recovery losses leading to low conversion efficiency is another concern [5].

To increase conversion efficiency and voltage gain, many high step-up converter topologies have been proposed. It is well known that the method of cascading several conventional boost converters may lead to low efficiency and high cost. And ensuring the stability of the cascaded converter is another concern. Several high set-up converter topologies that use coupled inductors are proposed for the FC generation system [6]–[9]. Although a high voltage gain is obtained, their efficiencies are degraded due to the losses associated with leakage inductances. And coupled inductors may bring in high switch voltage stress and EMI problems. The voltage-lift technique is an effective method that can be applied in electronic circuit designs, to attain a high voltage gain [10], [11]. It is, however, limited. A step-up converter based on charge pumps with one inductor inserted is proposed [12]. Unfortunately, its control circuit is usually difficult to design and the input current is not continuous, which is not a good choice for the PVs and FCs. The study in [13] has achieved a high voltage gain with continuous input current and a simple control circuit. But large switch voltage stress becomes one concern. The study in [14] and [15] proposes an effective topology that can achieve high voltage gains without high duty-cycle by cascading several voltage multiplier cells, whereas the high output voltage is achieved through lifting capacitor voltage step by step, making the capacitor voltage of the latter cell larger than that of the former cell. High voltage stress of the capacitors, increasing size and cost of converters, should be also taken into account.

To integrate different energy sources well and achieve high voltage gain, one possible solution to this problem is the application of the switched-capacitor technique on classical nonisolated dc–dc converters [16]–[21]. Based on it, a parallel switched-diode-capacitor voltage accumulator (SDCVA) composed of several switched-diode-capacitor cells in parallel and a serial

Manuscript received June 26, 2014; revised January 2, 2015 and October 6, 2014; accepted January 24, 2015. Date of publication February 18, 2015; date of current version September 21, 2015. This work was supported in part by National "111" Project, China, under Grant B08036, and in part by Chongqing Graduate Student Research Innovation Project, China, under Grant CYB14015. Recommended for publication by Associate Editor R. Zane.

The authors are with the State Key Laboratory of Power Transmission Equipment & System Security and New Technology, College of Electrical Engineering, Chongqing University, Chongqing 400044, China (e-mail: cjf6221@gmail.com; suntao@cqu.edu.cn; bixiaohuiq@163.com).

Color versions of one or more of the figures in this paper are available online at http://ieeexplore.ieee.org.

Digital Object Identifier 10.1109/TPEL.2015.2399853

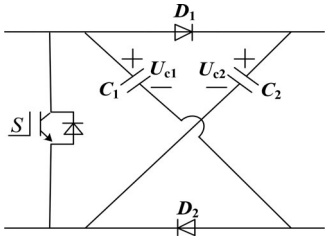

Fig. 1. Switched-diode-capacitor cell.

SDCVA composed of several switched-diode-capacitor cells in series are proposed in the paper. Then, a multi-input step-up converter based on the parallel SDCVA and a multi-input step-up converter based on the serial SDCVA are, respectively, presented. Both of them achieve a high voltage gain due to the accumulation of some or all capacitor voltages of SDCVA. Other advantages are included, such as low voltage stress and current stress across components, low voltage ripple and current ripple, and a simple control circuit. Furthermore, the proposed converters can be extended by simply increasing the number of switched-diode-capacitor cells.

II. Two SDCVA Structures

Fig. 1 shows the switched-diode-capacitor cell, which possesses a symmetrical characteristic as capacitors C_1, C_2 and diodes D_1, D_2 are, respectively, identical in technical parameters, making voltage across C_1 and C_2 equal

$$U_{c1} = U_{c2} \tag{1}$$

where U_{c1} and U_{c2} represent the voltage across C_1 and C_2, respectively.

The principle of the switched-diode-capacitor cell is that: when the main switch S is turned on, diodes D_1, D_2 are turned OFF with capacitors C_1, C_2 discharged in series; when S is turned OFF, diodes D_1, D_2 are turned ON with C_1, C_2 charged in parallel. A high voltage gain can be attained since two capacitors are discharged in series and charged in parallel automatically by the ON–OFF transition of the main switch.

Based on the switched-diode-capacitor cell, two different SDCVA structures could be attained: the first one called the parallel SDCVA consists of two switched-diode-capacitor cells in parallel, shown in Fig. 2(a); the second one called the serial SDCVA is composed of two switched-diode-capacitor cells in series, shown in Fig. 2(b). In the two SDCVA structures, the two switched-diode-capacitor cells are, respectively, labeled as cell 1, cell 2 and the capacitor voltage of each cell is, respectively, labeled as U_1, U_2. It should be noted that the two adjacent switched-diode-capacitor cells share the same diode D_2 in Fig. 2(a), and it is the reuse of the diode that makes the capacitor voltages of cell 1 and cell 2 equal, which can be verified by (5).

The two SDCVA structures can be utilized to construct two different double-input step-up converters, shown as follows.

1) The parallel SDCVA with two input ports in Fig. 2(a) can be utilized to construct a double-input converter with a high voltage gain, which feeds power to the load individually. It should be noted that the word "individually" in the paper means that the double-input converter operates with the two input sources alternately but only one of them is active every time. The two switches driven by the same switching signal provide a pathway for making two cells connected in parallel and a pathway for three capacitors of the parallel SDCVA connecting in series to feed the load power energy. A great advantage is that the same output effect will be attained when each input source works independently, namely, a double-input step-up converter for individual supplying power can be constructed based on the parallel SDCVA.
2) The serial SDCVA with two input ports in Fig. 2(b) can be used to build another double-input converter, which also achieves a high voltage gain. Different from the parallel SDCVA, the serial SDCVA is the circuit structure that can be used to build a double-input step-up converter for both simultaneous and individual supplying power. Also, the two switches are driven by a switching signal. However, the two switches make two capacitors of each cell in parallel and provide a pathway for making all rather than three capacitors of the serial SDCVA be connected in series to feed the load.

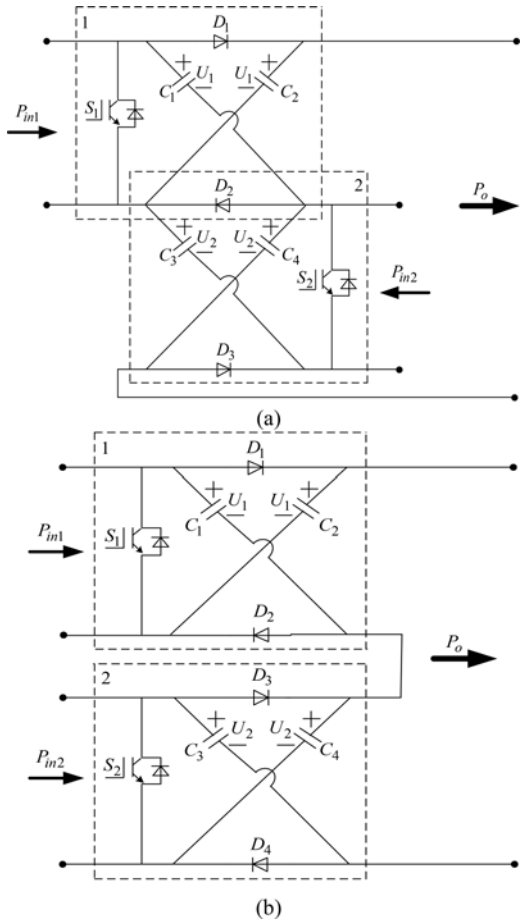

Fig. 2. Two SDCVA structures: (a) parallel SDCVA and (b) serial SDCVA.

Both the two proposed converters achieve a high voltage gain due to the boost circuit and the SDCVA, in which the boost circuit converts the low input voltage to a high voltage level

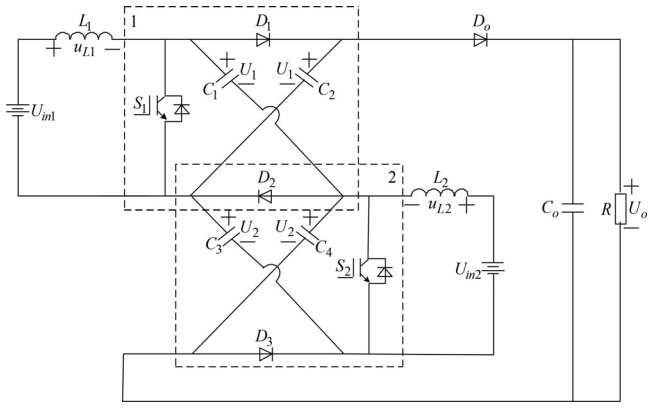

Fig. 3. Double-input step-up converter based on the parallel SDCVA.

and the SDCVA converts the high voltage level to a higher level simultaneously. It should be noted that the two converting processes are performed at the same time, i.e., it is a one-stage circuit instead of a two-stage circuit. Other outstanding merits are included as follows:

1) a high voltage gain can be achieved due to the accumulation of some or all capacitor voltages of SDCVA;
2) voltage stresses across all components of the two cells are equal and small, therefore, low voltage devices with small RS-ON can be adopted to reduce conduction loss and cost of the proposed converters.
3) a simple control circuit is attained since the two main switches are driven by the same switching signal;
4) high conversion efficiency is achieved.

This paper is organized as follows. Basic operation principle and performance analysis for the double-input step-up converter based on the parallel SDCVA and the double-input step-up converter based on the serial SDCVA are, respectively, presented in Sections III and IV. Section V shows the experimental verification in detail. Finally, a conclusion for the two converters is given in Section VI.

III. Double-Input Step-Up Converter Based on the Parallel SDCVA

Topology and operation principle of the double-input step-up converter based on the parallel SDCVA at the mode of individual supplying power are given in Section III-A. And the performance analysis of it is presented in the Section III-B. In addition, the converter can also operate at the mode of simultaneous supplying power. At this mode, the parallel SDCVA is a good choice to construct a novel voltage balance converter.

A. Operation Principle

Fig. 3 shows the basic topology of the double-input converter based on the parallel SDCVA, which is made of two switched-diode-capacitor cells in parallel. In the circuit topology, two switched-diode-capacitor cells are, respectively, labeled as cell 1, cell 2, and the two input sources are respectively labeled as input source 1, input source 2. Cell 1 and cell 2 share the same diode D_2. As the converter feeds power to the load R

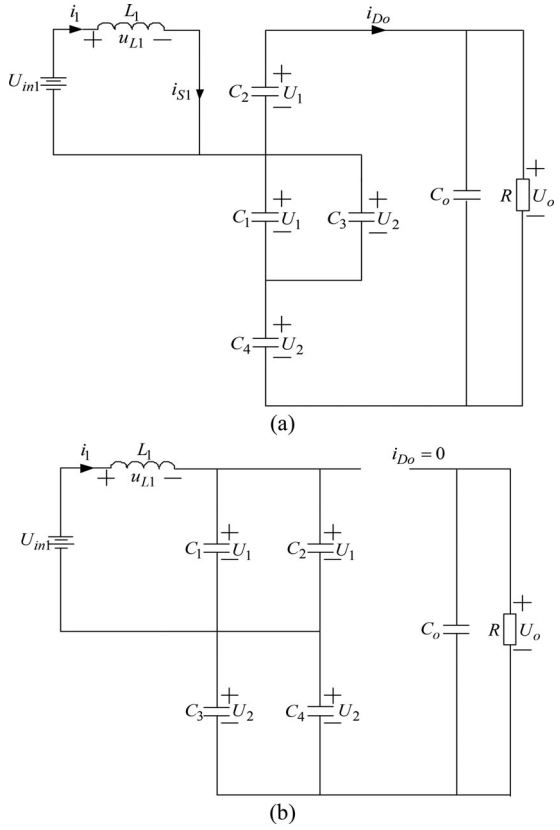

Fig. 4. Equivalent circuits when input source 1 works independently: (a) stage 1 and (b) stage 2.

individually, the specific two analysis processes when input source 1 and input source 2, respectively, work independently are presented next.

1) When Input Source 1 Works Independently: Equivalent circuits of the converter based on the parallel SDCVA when only input source 1 works independently are given in Fig. 4, including two operating stages.

Stage 1: When switches S_1 and S_2 are turned ON [see Fig. 4(a)], diodes D_1, D_2, and D_3 are reverse-biased while diode D_o is forwarded. During the switch-on period, capacitors C_1, C_2, C_3, and C_4 are under serial-and-parallel connection, where C_1, C_3 in parallel are connected with C_2 and C_4 in series. Thus, the capacitor voltage of cell 1 equals to the capacitor voltage of cell 2, i.e., U_1 equals to U_2. And it gives the reason why the SDCVA in Fig. 2(a) is called the parallel SDCVA. At this period, the voltage across the inductor L_1 can be obtained

$$u_{L1} = U_{\text{in}1}. \tag{2}$$

In the serial–parallel pathway of capacitors C_1–C_4, the output voltage is achieved as U_1+2U_2 or $2U_1+U_2$

$$U_o = U_1 + 2U_2 = 2U_1 + U_2. \tag{3}$$

Stage 2: When switches S_1 and S_2 are turned OFF [see Fig. 4(b)], diodes D_1, D_2, and D_3 are forwarded while diode D_o is reverse-biased. During the switch-off period, capacitors C_1, C_2 of cell 1 and capacitors C_3, C_4 of cell 2 are, respectively, connected in parallel, making each capacitor voltage of each

cell equal. The voltage across the inductor L_1 is written by

$$u_{L1} = U_{\text{in1}} - U_1. \tag{4}$$

In addition, by applying the principle of voltage–second balance on the inductor L_1 according to (2)–(4), we attain the capacitor voltage of the parallel SDCVA and the output voltage of the double-input step-up converter based on the parallel SDCVA as follows:

$$U_1 = U_2 = \frac{1}{1-D}U_{\text{in1}} \tag{5}$$

$$U_o = \frac{3}{1-D}U_{\text{in1}}. \tag{6}$$

2) When Input Source 2 Works Independently: Operation principle of the converter based on the parallel SDCVA when input source 2 works independently is similar to that when input source 1 works independently. Therefore, it is easy to obtain the capacitor voltage and the output voltage of the converter as follows:

$$U_1 = U_2 = \frac{1}{1-D}U_{\text{in2}} \tag{7}$$

$$U_o = \frac{3}{1-D}U_{\text{in2}}. \tag{8}$$

According to the double-input converter, it is not difficult to derive the voltage gain of *N*-input converter with *N* cells in parallel, which is given in the following equation:

$$\frac{U_o}{U_{\text{in}i}} = \frac{N+1}{1-D} \quad (i = 1, 2..., N). \tag{9}$$

B. Performance Analysis

As the converter could attain a similar output effect no matter which input source works independently, the operating mode when input source 1 works independently is taken as an example, to do detailed performance analysis later. First, the transient characteristic of the converter is analyzed in detail. Then, the current ripple, voltage ripple, voltage stress, and current stress are, respectively, discussed.

1) Transient Circuit Characteristic: Some definitions are given

$$\begin{array}{ll} C_1 = C_2 = C_3 = C_4 = C & U_1 = U_2 = U_c \\ I_{1\min} = I_1 - \Delta i_1 & I_{1\max} = I_1 + \Delta i_1 \\ U_{c\min} = U_c - \Delta u_c & U_{c\max} = U_c + \Delta u_c \end{array} \tag{10}$$

where the four capacitors C_1–C_4 have the same capacitance C, U_c represents the capacitor voltage value of the parallel SDCVA, $U_{c\min}, U_{c\max}$ represent the minimum value and maximum value of the capacitor voltage, Δu_c represents the capacitor voltage ripple, I_1 represents the average current of the inductor L_1, and $I_{1\min}$ and Δi_1, respectively, represents the minimum value of I_1 and the current ripple of the inductor L_1.

During the stage 1, U_{in1} is applied to the inductor L_1 and the input current i_1 can be written by

$$i_1 = I_{1\min} + \frac{U_{\text{in1}}}{L_1}t = I_1 - \Delta i_1 + \frac{U_{\text{in1}}}{L_1}t. \tag{11}$$

During the switch-on interval, the four capacitors C_1–C_4 construct a serial–parallel configuration, in which three capacitors (C_2, C_1, C_4 or C_2, C_3, C_4) are connected in series to realize accumulation of the three transient capacitor voltages. The equivalent capacitance of the serial–parallel configuration can be achieved by 2/5*C*, since the four capacitors have the same capacitance *C*. Thus, three expressions can be given

$$u_o = 3u_c \tag{12}$$

$$R\left(i_{Do} - C_{\text{o}}\frac{du_o}{dt}\right) = u_o \tag{13}$$

$$i_{Do} = -\frac{2}{5}C\frac{du_c}{dt} \tag{14}$$

where u_o, u_c, and i_{Do}, respectively, represent the transient output voltage of the converter, transient capacitor voltage of C_1–C_4, and the transient current through the diode D_o. In addition, the initial value of u_c during the stage 1 is $U_{c\max}$. From (12) to (14), the transient capacitor voltage u_c can be achieved as follows:

$$u_c = U_{c\max}e^{-\frac{15}{R(2C+15C_{\text{o}})}t}. \tag{15}$$

Then, i_{Do} can be further obtained based on (14):

$$i_{Do} = \frac{6CU_{c\max}}{R(2C+15C_{\text{o}})}e^{-\frac{15}{R(2C+15C_{\text{o}})}t}. \tag{16}$$

During the stage 2, U_{in1}–U_c is applied to the inductor L_1 and we have the input current i_1 expressed in

$$i_1 = I_{1\max} + \frac{U_{\text{in1}} - U_c}{L_1}t = I_1 + \Delta i_1 + \frac{U_{\text{in1}} - U_c}{L_1}t \tag{17}$$

where the initial value of i_1 during the stage 2 is $I_{1\max}$.

The input terminal of the circuit forms a current loop L_1–C_1–U_{in1}, which is described by

$$L_1\frac{di_1}{dt} + u_c = U_{\text{in1}}. \tag{18}$$

As the two capacitors of each cell are connected in parallel, the input current i_1 can be also written as follows:

$$i_1 = 2C\frac{du_c}{dt}. \tag{19}$$

By substituting (19) into (18), a second-order differential equation is obtained

$$2L_1C\frac{d^2u_c}{dt} + u_c = U_{\text{in1}} \tag{20}$$

where the initial value of u_c during the stage 2 is $U_{c\min}$.

During the switch-off period, the capacitor voltage u_c in each cell can be derived from (17) to (20)

$$u_c = (U_{c\min} - U_{\text{in1}})\cos\left(\sqrt{\frac{1}{2L_1C}}t\right) + \sqrt{\frac{L_1}{2C}}I_{1\max}\sin\left(\sqrt{\frac{1}{2L_1C}}t\right) + U_{\text{in1}}. \tag{21}$$

In addition, as the diode D_o is reverse-biased, the current i_{Do} flowing through the diode D_o is zero.

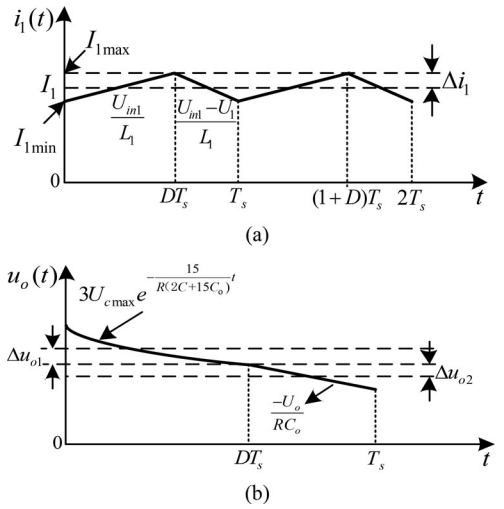

Fig. 5. Key waveforms: (a) input inductor current and (b) output voltage.

2) Current Ripples and Voltage Ripples: In the steady state of the converter, waveform of input inductor current i_1 is given in Fig. 5(a). It is easy to attain the current ripple of the input inductor L_1, which is also the input current ripple Δi_1

$$\Delta i_1 = \frac{U_{\rm in1}}{2L_1} DT_s. \tag{22}$$

According to (22), the expression of input current ripple is similar to that of the conventional boost converter.

In addition, according to the definitions mentioned in (10), the four capacitors have the same capacitance *C*. An equation can be obtained based on the energy conservation principle

$$\frac{3 \bullet \frac{1}{2}C(U_{c\max}^2 - U_{c\min}^2)}{T_s} = \frac{3C(U_{c\max}+U_{c\min})(U_{c\max}-U_{c\min})}{2T_s} = \frac{U_o^2}{R}. \tag{23}$$

In addition,

$$U_{c\max} + U_{c\min} = 2U_c. \tag{24}$$

Thus, the capacitor voltage ripples $\Delta u_1,\ \Delta u_2$ of the two cells can be formulated based on (23) and (24)

$$\Delta u_1 = \Delta u_2 = \frac{U_{c\max}-U_{c\min}}{2} = \frac{3U_{\rm in1}T_s}{2(1-D)RC}. \tag{25}$$

Though the SDCVA is combined with the conventional boost converter, the output voltage waveform of the converter shown in Fig. 5(b) is quite different from that of the conventional boost converter. In the conventional boost converter, the output filter capacitor delivers power to the load during switch-on period and input source and input inductor supply power to the load during switch-off period. However, in the proposed double-input step-up converter based on the parallel SDCVA, three capacitors of the parallel SDCVA are connected in series to feed the load during the switch-on period and the output filter capacitor delivers power to the load during the switch-off period. That is to say, during a whole switching period, the load is always charged by capacitors. As a result, the output voltage ripple can be divided into two different parts: voltage ripple Δu_{o1} during the switch-on period and voltage ripple Δu_{o2} during the switch-off period. Thereinto, Δu_{o1} could be derived by approximate calculation

$$\begin{aligned}\Delta u_{o1} &= \frac{1}{2}\left(3U_{c\max} - 3U_{c\max}e^{-\frac{15DT_s}{R(2C+15C_o)}}\right)\\ &= \frac{3}{2}U_{c\max}\left(1-e^{-\frac{15DT_s}{R(2C+15C_o)}}\right).\end{aligned} \tag{26}$$

As only the capacitor C_o feeds power to the load during the switch-off period, it is easy to attain the output voltage ripple Δu_{o2} during the switch-off period as follows:

$$\Delta u_{o2} = \frac{(1-D)U_oT_s}{2RC_o}. \tag{27}$$

Thus, the output voltage ripple Δu_o can be written by

$$\begin{aligned}\Delta u_o &= \Delta u_{o1} + \Delta u_{o2}\\ &= \frac{3}{2}U_{c\max}\left(1-e^{-\frac{15DT_s}{R(2C+15C_o)}}\right) + \frac{(1-D)U_oT_s}{2RC_o}.\end{aligned} \tag{28}$$

3) Component Stress: In the parallel SDCVA, all switches and diodes are subjected to a low voltage stress, which is described by the product of the input source voltage and 1/(1–*D*). Combining (5) and (7), it is clear to know that the capacitors have the same voltage stress as the switches and diodes. As a result, small and equal voltage stress of switches, diodes, and capacitors enables the use of the components with a low rated voltage and low RDS-ON, which greatly reduces losses.

Combing (11), (16), (17), and (22), the input inductor current i_1 and the current $i_{\rm Do}$ through the diode D_o can be, respectively, described as (29) see at the bottom of the page

$$i_1 = \begin{cases}\dfrac{3U_o}{(1-{\rm D})\rm R} - \dfrac{U_{\rm in1}}{2L_1}DT_s + \dfrac{U_{\rm in1}}{L_1}t & 0 < t \le DT_s\\ \dfrac{3U_o}{(1-{\rm D})\rm R} + \dfrac{U_{\rm in1}}{2L_1}DT_s - \dfrac{DU_{\rm in1}}{(1-D)L_1}(t-DT_s) & DT_s < t \le T_s\end{cases} \tag{29}$$

$$i_{Do} = \begin{cases}\dfrac{6CU_{c\max}}{R(2C+15C_o)}e^{-\frac{15}{R(2C+15C_o)}t} & 0 < t \le DT_s\\ 0 & DT_s < t \le T_s.\end{cases} \tag{30}$$

From (29), we know that the current stress $I_{\rm ipS1}$ of the switch S_1 can be achieved at the end of the switch-on interval

$$i_{{\rm ip}S1} = \frac{3U_o}{(1-{\rm D})\rm R} + \frac{U_{\rm in1}}{2L_1}DT_s \tag{31}$$

And from (30), the current stress $i_{\rm ipDo}$ of the diode D_o can be achieved at the beginning of the switch-on interval

$$i_{{\rm ip}Do} = \frac{6\,CU_{c\max}}{R\,(2\,C+15\,C_{\rm o})}. \tag{32}$$

At the same time, during the switch-off period, the current i_{S2} through the switch S_2 and the current through every diode

of the parallel SDCVA can be derived based on (21)

$$i_{D1} = i_{D2} = i_{D3} = i_{S2} = \mathrm{C}\frac{du_c}{dt} = \frac{I_{1\max}}{2C}\cos\left(\frac{1}{\sqrt{2L_1C}}t\right) - \frac{U_{c\min} - U_{\mathrm{in}1}}{\sqrt{2L_1C}}\sin\left(\frac{1}{\sqrt{2L_1C}}t\right). \quad (33)$$

Referring to (31)–(33), it is clear that the main switch S_1 is subjected to a relatively high current stress while the switch S_2 and the diodes of the SDCVA are all subjected to a low current stress. Low voltage stresses and current stresses across components greatly reduce the conduction losses.

In conclusion, the output effect is similar when each input source independently feeds power to the load. When one input source is active, the input power will be transferred into its own corresponding switched-diode-capacitor cell and the energy stored in the cell will be simultaneously transferred into its adjacent cell. Finally, all capacitors of the parallel SDCVA own the same capacitor voltage, i.e., the parallel SDCVA has the voltage self-balanced function. In addition, a high output voltage can be achieved by the accumulation of three capacitor voltages in the parallel SDCVA. Most importantly, the capacitor voltage of each cell is equal and small with the value $1/3U_o$, which is the biggest difference compared with the cascade step-up converters based on diode-capacitor voltage multiplier cells [17]. In the cascade step-up converters, as the capacitor voltage of the latter diode-capacitor cell is $1/(1–D)U_{\mathrm{in}}$ bigger than that of the former diode-capacitor cell, capacitors with high rated voltage should be needed. However, in the proposed double-input step-up converter based on the parallel SDCVA, small and equal capacitor voltage allows the use of capacitors with smaller voltage stress, reducing size and cost of the converter. Moreover, compared with the ones obtained by simply placing the output terminals of several converters in parallel or in series, another advantage of the proposed converter is that two cells operate all the time and make a contribution to achieving a very high voltage gain no matter which input source works independently. Thus, a high component utilization can be achieved.

C. Novel Voltage Balance Converter

As analyzed previously, the converter based on the parallel SDCVA operates at the mode of individual supplying power where the two input sources works alternately. If the converter operates at the mode of simultaneous supplying power, the two input sources will have the same voltage value due to the automatic voltage self-balanced function of the parallel SDCVA. And it is just this function that makes the parallel SDCVA a good choice to construct a novel voltage balance converter, which is suitable for a serial battery string.

The operation principle of the voltage balance converter is that: when two input sources work simultaneously, the two cells work alternatively between charging and discharging states, making the excess energy transferred from the input source with high voltage to the input source with low voltage. And finally, both of the two input sources achieve the same voltage value. Unlike the traditional voltage balance converter, all batteries in the proposed converter with simultaneous supplying power are not connected in series directly. Conversely, they are connected in series with the parallel SDCVA indirectly, in which separate batteries serve as the multiple input sources. And the output voltage of the self-balanced converter for N batteries is the product of $(N+1)/(1–D)$ and the self-balanced voltage. In addition, a great advantage of the voltage self-balanced converter is that when some battery is out of service, the converter can still complete the voltage self-balanced function for the other batteries and the output voltage keeps unchanged.

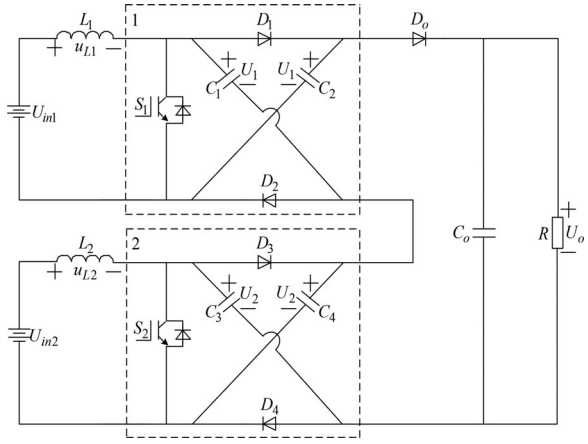

Fig. 6. Double-input step-up converter based on the serial SDCVA.

IV. Double-Input Step-Up Converter Based on the Serial SDCVA

Another double-input step-up converter based on the serial SDCVA is proposed in this section. The converter can also feed load individually as well as simultaneously. Operation principle and performance analysis are, respectively, given.

A. Operation Principle

Fig. 6 shows the basic topology of the double-input step-up converter based on the serial SDCVA, which consists of two switched-diode-capacitor cells in series. In the converter, the operating mode of simultaneous supplying power and the operating mode of individual supplying power are, respectively, presented next.

1) Operating Mode of Simultaneous Supplying Power: Equivalent circuits of the converter when two input sources work simultaneously are presented in Fig. 7, including two operating stages. Some definitions are given as follows:

$$C_1 = C_2 = C_{\mathrm{cell}1} \qquad C_3 = C_4 = C_{\mathrm{cell}2}. \quad (34)$$

Stage 1: When switches S_1, S_2 are turned ON [see Fig. 7(a)], the voltage across inductor L_1 and the voltage across inductor L_2 can be formulated in

$$u_{Li} = U_{\mathrm{in}i} \quad (i = 1,\ 2). \quad (35)$$

Since all capacitors of the SDCVA are connected in series to feed the load, the output voltage of the converter based on the serial SDCVA can be written by

$$U_o = 2U_1 + 2U_2. \quad (36)$$

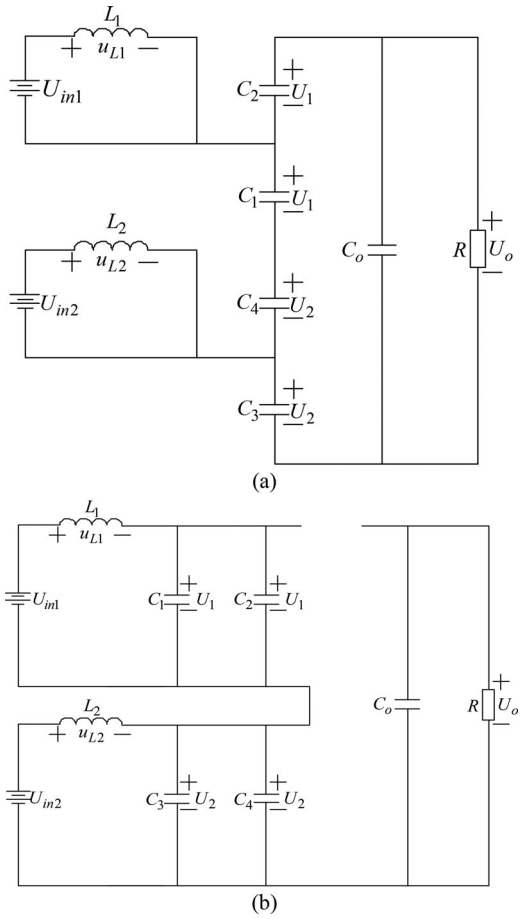

Fig. 7. Equivalent circuits when the converter is under the operating mode of simultaneous supplying power: (a) stage 1 and (b) stage 2.

Stage 2: When switches S_1, S_2 are turned OFF [see Fig. 7(b)], capacitors C_1, C_2 of cell 1 and capacitors C_3, C_4 of cell 2 are, respectively, connected in parallel, making each capacitor voltage of each cell equal. During this period, the voltages across L_1 and L_2 are, respectively, expressed as follows:

$$u_{Li} = U_{\text{in}i} - U_i \quad (i = 1,\ 2). \tag{37}$$

From (35) to (37), we obtain the following results:

$$U_i = \frac{1}{1-D} U_{\text{in}i} \quad (i = 1,\ 2) \tag{38}$$

$$U_o = \frac{2}{1-D}(U_{\text{in}1} + U_{\text{in}2}). \tag{39}$$

Similarly, it is easy to conclude the output voltage of the *N*-input converter for simultaneous supplying power, which is formulated in the following equation:

$$U_o = \frac{2}{1-D} \sum_{i=1}^{N} U_{\text{in}i}. \tag{40}$$

2) Operating Mode of Individual Supplying Power: In the operating mode of individual supplying power, the two input sources of the converter work alternately. When the input source 1 works, only cell 1 makes a contribution to boosting the low input voltage to the value 2/(1–*D*)$U_{\text{in}1}$ and cell 2 continues to work to provide a pathway for the boosting process. When the input source 2 works, only cell 2 makes a contribution to boosting the low input voltage to the value 2/(1–*D*)$U_{\text{in}2}$ and cell 1 continues to work to provide a pathway for the boosting process. Compared with (6) and (8), the voltage gain of the converter operating at the mode of individual supplying power is 1/(1–*D*) smaller than that of the double-input converter based on the parallel SDCVA.

B. Performance Analysis

1) Component Voltage Stress: The component voltage stress of cell 1 is described by

$$\begin{aligned} u_{vpS1} &= u_{vpC1} = u_{vpC2} = u_{vpD1} = u_{vpD2} \\ &= \frac{1}{1-D} U_{\text{in}1} \end{aligned} \tag{41}$$

where u_{vpS1}, u_{vpC1}, u_{vpC2}, u_{vpD1}, and u_{vpD2}, respectively, represent the voltage stress across S_1, C_1, C_2, D_1, and D_2 of cell 1.

The component voltage stress of cell 2 is described by

$$\begin{aligned} u_{vpS2} &= u_{vpC3} = u_{vpC4} = u_{vpD3} = u_{vpD4} \\ &= \frac{1}{1-D} U_{\text{in}2} \end{aligned} \tag{42}$$

where u_{vpS2}, u_{vpC3}, u_{vpC4}, u_{vpD3}, and u_{vpD4}, respectively, represent the voltage stress across S_2, C_3, C_4, D_3, and D_4 of cell 2. In addition, the voltage stress across the diode D_o is as follows:

$$u_{vpDo} = \frac{1}{1-D} U_{\text{in}1} + \frac{1}{1-D} U_{\text{in}2} = \frac{1}{2} U_o. \tag{43}$$

According to (41)–(43), it is clear to know that the voltage stresses of the main switch, capacitors, and diodes of each cell are equal and small, which can be described by the product of the corresponding input source voltage and 1/(1–*D*). And the voltage stress across D_o is only half of the output voltage.

2) Current Ripples and Voltage Ripples: In the converter based on the serial SDCVA, the current ripples of L_1 and L_2 can be described in

$$\Delta i_i = \frac{U_{\text{in}i}}{2L_i} D T_s \quad (i = 1,\ 2). \tag{44}$$

As the two input sources work together in series, their average input currents are equal

$$I_1 = I_2. \tag{45}$$

In addition, by applying the energy conservation principle, we attain

$$I_1 U_{\text{in}1} + I_2 U_{\text{in}2} = \frac{U_o^2}{R}. \tag{46}$$

Combining (39), (45), and (46), two average input currents are achieved as follows:

$$I_1 = I_2 = \frac{2U_o}{(1-D)R}. \tag{47}$$

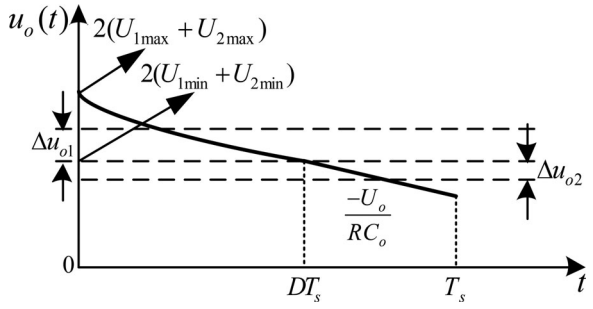

Fig. 8. Output voltage waveform.

Some definitions are given

$$\begin{array}{ll} U_{1\min}=U_1-\Delta u_1 & U_{1\max}=U_1+\Delta u_1 \\ U_{2\min}=U_2-\Delta u_2 & U_{2\max}=U_2+\Delta u_2 \\ C_1=C_2=C_{\text{cell1}} & C_3=C_4=C_{\text{cell2}} \end{array} \tag{48}$$

where $U_{1\min}$ and $U_{1\max}$, respectively, represent the minimum value and maximum value of capacitor voltage of cell 1, $U_{2\min}$ and $U_{2\max}$ represent the minimum value and maximum value of capacitor voltage of cell 2, and Δu_1 and Δu_2 represent the capacitor voltage ripples of cell 1 and cell 2.

In terms of the capacitor voltage of cell 1, an equation can be obtained by applying the energy conservation principle

$$2 \bullet \frac{1}{2} C_{\text{cell1}} (U_{1\max}^2 - U_{1\min}^2)/T_s = U_{\text{in1}} I_1. \tag{49}$$

In addition, the minimum value and the maximum value of the capacitor voltage of cell 1 have the relation as follows:

$$U_{1\max} + U_{1\min} = 2U_1. \tag{50}$$

By substituting (50) into (49), the capacitor voltage ripple of cell 1 can be attained as follows:

$$\Delta u_1 = \frac{U_{1max} - U_{1\min}}{2} = \frac{U_o T_s}{2RC_{\text{cell1}}}. \tag{51}$$

By applying the previous computing method, the capacitor voltage ripple of cell 2 can be attained as follows:

$$\Delta u_2 = \frac{U_{2\max} - U_{2\min}}{2} = \frac{U_o T_s}{2RC_{\text{cell2}}}. \tag{52}$$

Like the double-input step-up converter based on the parallel SDCVA, the load of the converter based on the serial SDCVA is always charged by capacitors. Therefore, the output voltage ripple can also be divided into two different parts: voltage ripple Δu_{o1} during the switch-on interval and voltage ripple Δu_{o2} during the switch-off interval, shown in Fig. 8. A little difference is that during the switch-on interval, the load of the converter based on the serial SDCVA is fed by all capacitors while the load of the converter based on the parallel SDCVA is fed by three capacitors.

During the switch-on period, as the output voltage equals to the accumulation of all capacitor voltages, it reaches the maximum value $2(U_{1\max}+U_{2\max})$ at the beginning of the switch-on period and the minimum value $2(U_{1\min}+U_{2\min})$ at the end of the the switch-on period. Combining (49) and (50), the voltage ripple Δu_{o1} during the switch-on period could be achieved

$$\begin{aligned} \Delta u_{o1} &= \frac{2(U_{1\max}+U_{2\max}) - 2(U_{1\min}+U_{2\min})}{2} \\ &= \frac{U_o T_s}{RC_{\text{cell1}}} + \frac{U_o T_s}{RC_{\text{cell2}}}. \end{aligned} \tag{53}$$

Also, Δu_{o2} during the switch-off period could be easily deduced like (27)

$$\Delta u_{o2} = \frac{(1-D)U_o T_s}{2RC_o}. \tag{54}$$

Therefore, the output voltage ripple can be achieved

$$\begin{aligned} \Delta u_o = \ \Delta u_{o1} + \Delta u_{o2} &= \frac{U_o T_s}{RC_{\text{cell1}}} + \frac{U_o T_s}{RC_{\text{cell2}}} \\ &+ \frac{(1-D)U_o T_s}{2RC_o}. \end{aligned} \tag{55}$$

V. Comparative Analysis and Closed-Loop Control

A. Comparative Analysis

A comparison of voltage stresses among the two proposed converters and the traditional boost converter is presented in Table I. It can be seen from Table I that the voltage gains of the two proposed converters are both higher than that of the traditional boost converter. And in the double-input step-up converter based on the parallel SDCVA, the component voltage stress of each cell is the product of its corresponding input source voltage and 1/(1–*D*), which is also 1/3 of its output voltage. In addition, the voltage stress of the output diode D_o is also 1/3 of its output voltage. In the double-input step-up converter based on the serial SDCVA, the component voltage stress of each cell is the product of its corresponding input source voltage and 1/(1–*D*). And the component voltage stress of each cell and the voltage stress of the output diode D_o are all half of its output voltage. On the whole, if these three converters output the same voltage, the voltage stresses of all components of the proposed converters are smaller than that of the traditional boost converter. Low voltage stress across component will reduce cost and size of circuit designs.

B. Closed-Loop Control

As the two proposed converter topologies are similar, they can be designed in one variable-structure circuit presented in Fig. 9 by adding three toggle switches Q_1, Q_2, and Q_3. The two converter topologies can be transformed from one to the other by the ON–OFF transition of these three switches. When Q_1, Q_2 are both turned on and Q_3 is turned off, the circuit is equivalent to the circuit of the double-input step-up converter based on the parallel SDCVA. When Q_1, Q_2 are both turned off and Q_3 is turned on, the circuit is equivalent to the circuit of the double-input step-up converter based on the serial SDCVA. In the experimental prototype, these three switches are implemented based on toggle switches.

To make the proposed converters operate stably when the input voltage varies, a voltage closed-loop control is essential. Structure diagram of the voltage closed-loop control circuit for

TABLE I
COMPARISON OF VOLTAGE STRESSES AMONG THE TWO PROPOSED CONVERTERS AND THE TRADITIONAL BOOST CONVERTER

The proposed double-input step-up converters			Output voltage U_o	Voltage stress of switches, diodes, capacitors		
				Cell 1	Cell 2	D_o
The converter based on the parallel SDCVA	Individual/Simultaneous	Input source 1	$3U_{\text{in}1}/(1–D)$	$1/3\ U_o$	$1/3\ U_o$	$1/3\ U_o$
		Input source 2	$3U_{\text{in}2}/(1–D)$	$1/3\ U_o$	$1/3\ U_o$	$1/3\ U_o$
The converter based on the serial SDCVA	Simultaneous	Input sources 1, 2	$(2U_{\text{in}1}+2U_{\text{in}2})/(1–D)$	$U_{\text{in}1}/(1–D)$	$U_{\text{in}2}/(1–D)$	$1/2\ U_o$
	Individual	Input source 1	$2U_{\text{in}1}/(1–D)$	$1/2\ U_o$	–	$1/2\ U_o$
		Input source 2	$2U_{\text{in}2}/(1–D)$	–	$1/2\ U_o$	$1/2\ U_o$
Traditional boost converter			$U_{\text{in}}/(1–D)$	U_o		U_o

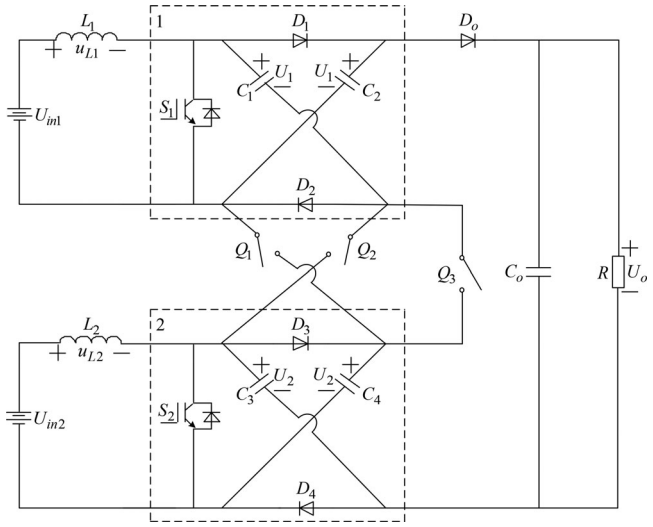

Fig. 9. Variable-structure circuit for the two proposed converters.

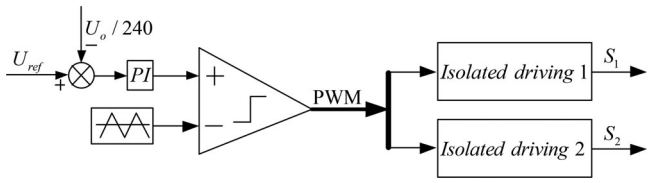

Fig. 10. Structure diagram of the voltage closed-loop control circuit.

the proposed converters is presented in Fig. 10, in which an a voltage error signal is obtained by taking the referring signal of the output voltage U_{ref} to subtract the sampling output voltage, which is designed to be U_o/240, and then passes through the proportional-integral regulator to compare with the carrier signal to achieve the driving signal for the two switches S_1, S_2. It should be noted that the driving signal must be isolated during the experimental research, because the switches S_1, S_2 do not share the same ground with the output port. But on the whole, the control circuit is simple and a stable output voltage can be obtained.

VI. EXPERIMENTAL VERIFICATION

The experimental prototype with output power 160 W for the two proposed converters is presented in Fig. 11(a). And the main components and parameters of the prototype are

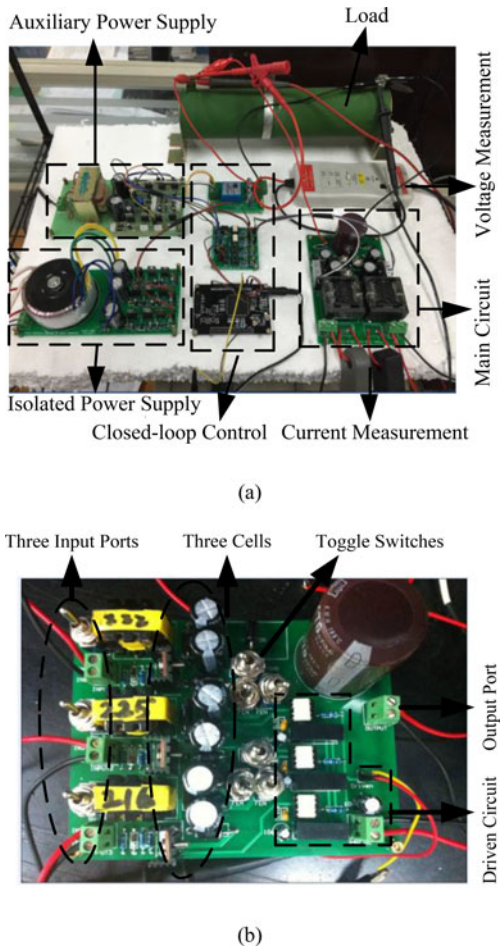

Fig. 11. Experimental prototypes: (a) proposed converter prototypes and (b) voltage balance circuit for three batteries.

summarized in Table II. In the prototype, the main circuit is realized based on the variable-structure circuit presented in Fig. 9, which can save the design cost. In addition, the voltage closed-loop control is realized based on the digital signal processor TMS320F2812, the voltage sampling circuit, and the isolated-driving circuit. The isolated power supply provides the voltages for the isolated-driving circuit, and the auxiliary power supply provides the voltages for the voltage sampling circuit. Furthermore, Fig. 11(b) presents the prototype of the three-input step-up converter based on the parallel SDCVA, which can realize the voltage self-balanced function for three batteries as

TABLE II
EXPERIMENTAL PARAMETERS

Components	Rated value
Switching frequency f_S	30 kHz
Inductors L_1, L_2 in Section III	900 μH
Inductors L_1, L_2 in Section IV	800 μH
Load R	1000 Ω
Control circuit	TMS320F2812
Optocoupler	TLP250
High frequency switches S_1, S_2	IRFP250
Switches Q_1, Q_2, Q_3	Toggle switch
Diodes D_1, D_2, D_3, D_4, D_5, D_6	MUR420
Output diode D_o	MUR440
Capacitors C_1, C_2, C_3, C_4, C_5, C_6	100 μF/250 V
Output filter capacitor C_o	470 μF/470 V
Three lead-acid rechargeable batteries	12 V/7 AH

well as achieving a high voltage gain. Though three inductors in the voltage balance circuit are designed to be 220 μH, they are, respectively, 222, 225, and 216 μH due to some deviations in fact.

In the section, the experimental results of the converter based on the parallel SDCVA and that of the converter based on the serial SDCVA are, respectively, given. It should be noted that $u_{Si}(i = 1, 2)$ is defined to describe the voltage difference between the drain terminal and the source terminal of the MOSFETs. And $u_{Di}(i = 1, 2, 3, 4)$ is defined to describe the voltage difference between the cathode and the anode of the diodes D_1-D_4. In addition, u_{Do} is given to describe the voltage difference between the cathode and the anode of the diode D_o.

A. Converter Based on the Parallel SDCVA

The converter is designed to operate stably with 400 V output voltage when the input voltage varies between 33 and 50 V. The experimental results when the input source 1 works independently are presented in Fig. 12, where (a), (b), and (c), respectively, shows the key waveforms when the input source 1 is, respectively, 33, 40, and 50 V. In addition, waveforms of all the components of the parallel SDCVA are presented in (d)–(f). To further analyze the dynamic performance of the converter, waveforms of the output voltage and the current of L_1 shown in (g) when the voltage of the input source 2 jumps from 33 to 40 V, and the waveforms shown in (h) when the voltage of the input source 2 jumps from 40 to 33 V are, respectively, presented. Furthermore, the experimental results when the input source 2 works independently are presented in Fig. 13, where (a) and (b) shows the key waveforms when the input source 1 is, respectively, 33 and 50 V.

On one hand, it cannot be difficult to see from Fig. 12 that the output voltage is stable with the value 398 V, getting close to the theoretical value 400 V, though the voltage of the input source 1 changes from 33 to 50 V. When the input voltage is 33 V in Fig. 12, the average current of the inductor L_1 is 5.16 A. While when the input voltage increases to 40 V, the average current is 4.23 A. And finally when the input voltage increases to 50 V, the average current is 3.39 A. Thus, the average input power is about 170 W and when the input voltage increases, the average

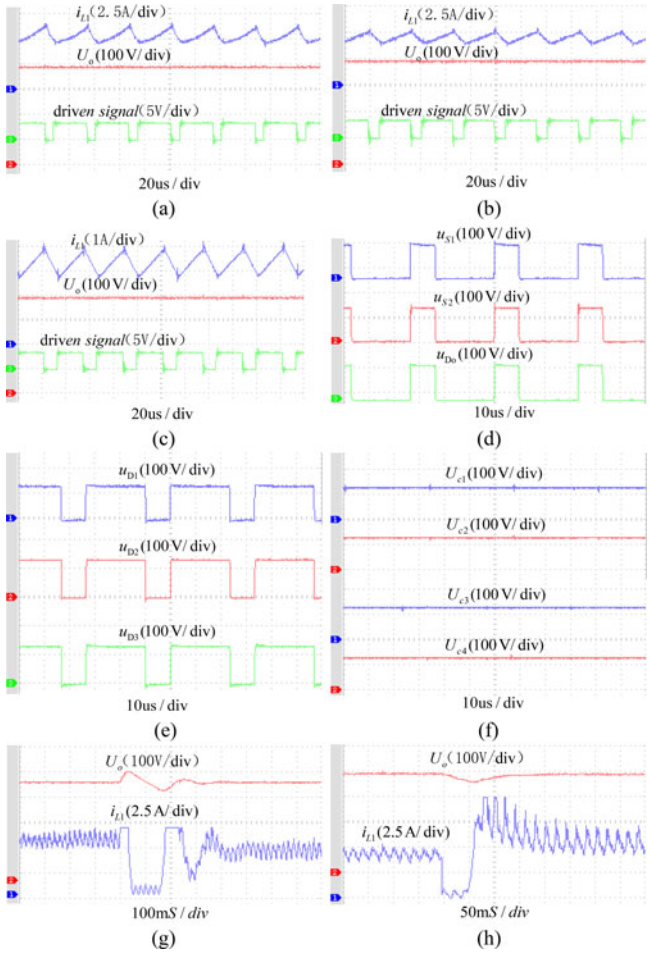

Fig. 12. Experimental results when the input source 1 works independently: (a) 33 V input voltage, (b) 40 V input voltage, (c) 50 V input voltage, (d) waveforms of S_1, S_2, and D_o, (e) waveforms of D_1, D_2, and D_3, (f) capacitor voltage waveforms, (g) input voltage jumps from 33 to 40 V, and (h) input voltage jumps from 40 to 33 V.

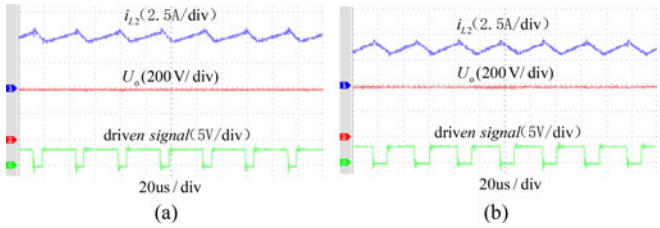

Fig. 13. Experimental results when the input source 2 works independently: (a) 33 V input voltage and (b) 50 V input voltage.

current of the inductor L_1 decreases to keep a stable output power 160 W. As a result, the conversion efficiency of the converter is as high as 94.1%. Furthermore, it can be seen from Fig. 12(d) and (e) that the top voltages of the MOSFETs S_1, S_2 and the four diodes D_o, D_1, D_2, and D_3 are nearly the same with the value 132 V. And from Fig. 12(f), we know that the four capacitors C_1, C_2, C_3, and C_4 also share the same average voltage with the value 133 V. Thus, the top voltages of the MOSFETs, diodes, and the average capacitor voltages are equal, which is nearly 1/3 of the output voltage. And the output voltage 398 V is nearly

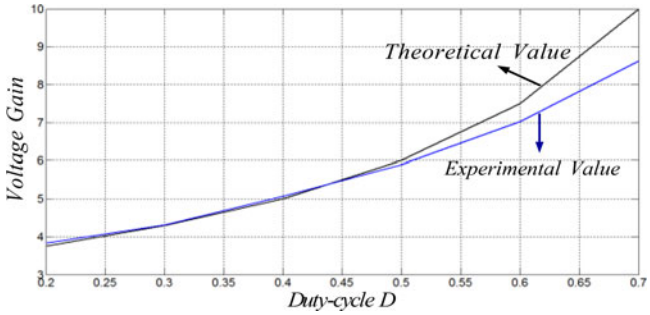

Fig. 14. Graph comparing theoretical and experimental voltage gains versus duty-cycle for the mode of individual supplying power when the input source 1 is active.

the accumulation of three capacitor voltages. In Fig. 12(g) and (h), it is obvious that the output voltage and the current of L_1 are regulated well with a short regulation time and low voltage overshoot.

On the other hand, it is easy to see from Fig. 13 that the similar results are achieved when the input source 2 works independently. And the conversion efficiency of the converter when the input source 2 works independently is also as high as 94.1%.

In conclusion, all experimental results indicate that the same output effects can be achieved no matter which input source is active in the double-input step-up converter based on the parallel SDCVA.

Fig. 14 shows the graph comparing theoretical and experimental voltage gains versus duty-cycle for the mode of individual supplying power when the input source 1 is active. It is easy to conclude that both the theoretical and experimental voltage gains increase with the duty-cycle increasing. And the experimental voltage gain approximates the theoretical voltage gain when the duty-cycle varies between 0.20 and 0.50. However, when the duty-cycle is over 0.50, the experimental voltage gain is less than the theoretical voltage gain and their voltage gain difference increases as the duty-cycle increases. This phenomenon may attribute to the variable input voltage and component losses. Fortunately, the voltage closed loop can relief it to some degree.

As analyzed in Section III-C, the converter based on the parallel SDCVA can also be utilized to construct a voltage balance system. In Fig. 11(b), a voltage balance prototype according to the three-input converter based on the parallel SDCVA has been built for the voltage balance of three batteries, whose initial voltages are, respectively, 11.770, 10.398, and 12.275 V. All batteries work simultaneously and about 180 min later; voltages of the three batteries are, respectively, 11.792, 11.695, and 11.884 V with the voltage difference of only 0.1 V among each other. And the balancing time is long, which may attribute to the large capacity of these batteries. Further researches for the voltage balance of batteries will be done in the future. For this research, three inductors in the voltage balance system will be substituted by three high frequency MOSFETs and then a modified system will be presented. Smaller size and cost will be achieved.

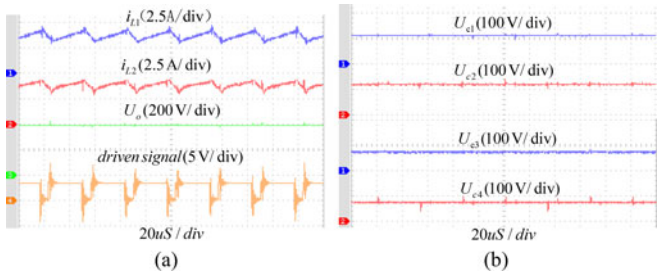

Fig. 15. Experimental results when $U_{\mathrm{in}1} = 30$ V, $U_{\mathrm{in}2} = 20$ V: (a) inductor currents, output voltage, and driving signal and (b) capacitor voltage.

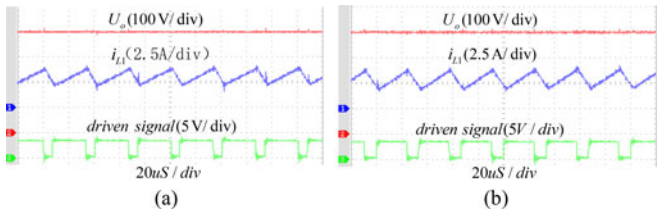

Fig. 16. Experimental results when the input source 1 works independently: (a) 50 V input and (b) 66 V input.

B. Converter Based on the Serial SDCVA

As analyzed in the Section IV-B, the double-input converter based on the serial SDCVA can work at both the modes of individual supplying power and simultaneous supplying power. Like the converter based on the parallel SDCVA, the converter based on the serial SDCVA is also designed to operate stably with 400 V output for the two modes.

In terms of the mode of simultaneous supplying power, experimental results when the two input sources are, respectively, 30 and 20 V, are presented in Fig. 15, including the waveforms of inductor currents, output voltage, and capacitor voltages. From these results, it is clear that the converter outputs a stable voltage 402 V, which basically matches its theoretical value 400 V. In addition, the average current of L_1 and the average current of L_2 are equal with the value 3.55 A, which verifies (45). Meanwhile, the conversion efficiency of the converter is 91.0%. In Fig. 15(b), the capacitor voltages of C_1 and C_2 are both 112 V, and the capacitor voltages of C_3 and C_4 are both 74 V. It can be known from the four capacitor voltages that every two capacitor voltages in the same switched-diode-capacitor cell are equal. The capacitor voltages of the two cells are different because the two input sources have different voltages. In particular, all the four capacitor voltages are small, compared with the high output voltage 402 V.

When the converter operates at the mode of individual supplying power, key experimental waveforms with 50 V input and 66 V input are, respectively, given in Figs. 16 and 17. When only the input source 1 is active, the output voltage is stable with the value 400 V. The average current of L_1 is 3.40 A when the input voltage is 50 V and 2.58 A when the input voltage is 66 V. Moreover, the conversion efficiency is as high as 94.1%. When only the input source 2 is active, the output voltage is also stable with the value 400 V, and the average current of L_2 is,

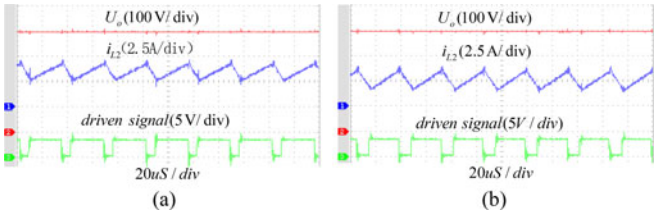

Fig. 17. Experimental results when the input source 2 works independently: (a) 50 V input and (b) 66 V input.

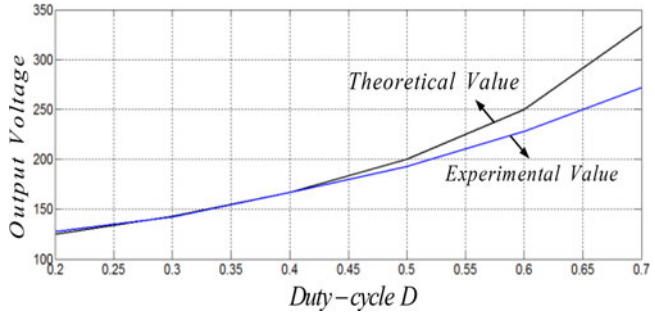

Fig. 18. Graph comparing theoretical and experimental voltage values versus duty-cycle for the mode of simultaneous supplying power when $U_{\mathrm{in}1} = 30$ V and $U_{\mathrm{in}2} = 20$ V.

respectively, 3.38 and 2.54 A when the input voltage is, respectively, 50 and 66 V. At this situation, the conversion efficiency is about 94.7%.

On the whole, the experimental results of the converter based on the serial SDCVA indicate that the two operating modes are feasible and the conversion efficiency of the converter is high.

Furthermore, the graph comparing theoretical and experimental voltage values versus duty-cycle for the mode of simultaneous supplying power is presented in Fig. 18. It is not difficult to conclude that the experimental output voltage basically matches the theoretical output voltage when the duty-cycle varies between 0.20 and 0.50. However, when the duty-cycle is over 0.50, the experimental output voltage value is less than the theoretical value, and their voltage difference increases with the duty-cycle increasing. This phenomenon is similar to that of the converter based on the parallel SDCVA. As analyzed before, it is normal since variable input voltage and component losses may result in voltage offsets.

As described in the experimental section, all experimental results are sufficient to verify the correctness of the theoretical analysis for the two proposed double-input step-up converters. Both the two converters can operate stably at the modes of individual supplying power and simultaneous supplying power with low component stresses, simple voltage closed-loop control, and high conversion efficiencies.

VII. Conclusion

In this paper, two SDCVA structures are proposed and then two different double-input step-up converters are, respectively, proposed based on them. According to theoretical analyses and experimental researches, we know that the proposed converters can achieve high voltage gains with low component stresses, simple control, and high conversion efficiencies. It should be emphasized that a high output voltage is achieved by the accumulation of three serial capacitor voltages in the double-input converter based on the parallel SDCVA operating at the mode of individual supplying power. Operating principle of the converter operating at this mode is that the input source delivers power to its corresponding switched-diode-capacitor cell and then the power stored in the cell is transmitted to its adjacent cell. Besides, the parallel SDCVA has the voltage self-balanced function that makes it a good choice to construct a novel voltage balance system for batteries with different voltages. In the system, the three-input converter based on the parallel SDCVA operates at the mode of simultaneous supplying power, where the three batteries with different voltages achieve the same voltage finally.

In addition, for the double-input step-up converter based on the serial SDCVA, the high output voltage is attained by the accumulation of all capacitor voltages of the serial SDCVA. Like the converter based on the parallel SDCVA, the converter based on the serial SDCVA can work at the modes of individual supplying power and simultaneous supplying power. When only one input source works independently, only the switched-diode-capacitor cell which is connected with the input source makes a contribution to the output voltage. So, the voltage gain of the converter operating at the mode of individual supplying power is less than that of the converter based on the parallel SDCVA.

Furthermore, all devices in the two SDCVA and the output diode D_o have low voltage stresses and current stresses. High conversion efficiencies have been achieved in both the two proposed converters. As the MICs are related to the energy management technique in renewable power generation area, great work combined with storage technique based on the proposed converters will be done further.

References

[1] F. Blaabjerg, Z. Chen, and S. B. Kjaer, "Power electronics as efficient interface in dispersed power generation systems," *IEEE Trans. Power Electron.*, vol. 19, no. 5, pp. 1184–1194, Sep. 2004.

[2] Y.-C. Liu and Y.-M. Chen, "A systematic approach to synthesizing multi-input DC-DC converters," *IEEE Trans. Power Electron.*, vol. 24, no. 1, pp. 116–127, Jan. 2009.

[3] A. Kwasinski, "Identification of feasible topologies for multiple-input DC-DC converters," *IEEE Trans. Power Electron.*, vol. 24, no. 3, pp. 856–861, Mar. 2009.

[4] S. Choi, V. G. Agelidis, J. Yang, D. Coutellier, and P. Marabeas, "Analysis, design and experimental results of a floating-output interleaved-input boost-derived DC-DC high-gain transformerless converter," *IET Power Electron.*, vol. 4, no. 1, pp. 168–180, 2011.

[5] D. Maksimovic and S. Cuk, "Switching converters with wide dc conversion range," *IEEE Trans. Power Electron.*, vol. 6, no. 1, pp. 151–157, Jan. 1991.

[6] S.-M. Chen, T.-J. Liang, L.-S. Yang, and J.-F. Chen, "A cascaded high step-up DC–DC converter with single switch for microsource applications," *IEEE Trans. Power Electron.*, vol. 26, no. 4, pp. 1146–1153, Apr. 2011.

[7] Y.-P. Hsieh, J.-F. Chen, T.-J. Liang, and L.-S. Yang, "Novel high step-up DC–DC converter with coupled-inductor and switched-capacitor techniques," *IEEE Trans. Ind. Electron.*, vol. 59, no. 2, pp. 998–1007, Feb. 2012.

[8] L.-S. Yang, T.-J. Liang, H.-C. Lee, and J.-F. Chen, "Novel high step-up DC–DC converter with coupled-inductor and voltage-doubler circuits," *IEEE Trans. Ind. Electron.*, vol. 58, no. 9, pp. 4196–4206, Sep. 2011.

[9] F. L. Tofoli, D. de Souza Oliveira, R. P. Torrico-Bascopé, and Y. J. A. Alcazar, "Novel nonisolated high-voltage gain DC-DC converters based on 3SSC and VMC," *IEEE Trans. Power Electron.*, vol. 27, no. 9, pp. 3897–3907, Sep. 2012.
[10] M. Zhu and F. L. Luo, "Voltage-lift-type Cuk converters: Topology and analysis," *IET Power Electron.*, vol. 2, no. 2, pp. 178–191, 2009.
[11] M. Zhu and F. L. Luo, "Series SEPIC implementing voltage-lift technique for DC-DC power conversion," *IET Power Electron.*, vol. 1, no. 1, pp. 109–121, 2008.
[12] K. I. Hwu and Y. T. Yau, "High step-up converter based on charge pump and boost converter," *IEEE Trans. Power Electron.*, vol. 27, no. 5, pp. 2484–2494, May 2012.
[13] M. Prudente, L. L. Pfitscher, G. Emmendoerfer, E. F. Romaneli, and R. Gules, "Voltage multiplier cells applied to non-isolated dc-dc converters," *IEEE Trans. Power Electron.*, vol. 23, no. 2, pp. 871–887, Mar. 2008.
[14] M. Prudente, L. L. Pfitscher, and R. Gules, "A boost converter with voltage multiplier cells," in *Proc. IEEE Power Electron. Spec. Conf.*, 2005, pp. 2716–2721.
[15] A. A. Fardoun and E. H. Ismail, "Ultra step-up DC-DC converter with reduced switch stress," *IEEE Trans. Ind. Appl.*, vol. 46, no. 5, pp. 2025–2034, Sep./Oct. 2010.
[16] A. Shenkman, Y. Berkovich, and B. Axelrod, "Novel AC-DC and DC-DC converters with a diode-capacitor SC multiplier," *IEEE Trans. Acrosp. Electron. Syst.*, vol. 40, no. 4, pp. 1286–1293, Oct. 2004.
[17] B. Axelrod, Y. Berkovich, and A. Ioinovici, "Switched-capacitor/switched-inductor structures for getting transformerless hybrid DC–DC PWM converters," *IEEE Trans. Circuits Syst.*, vol. 55, no. 2, pp. 687–696, Mar. 2008.
[18] B. Axelrod, Y. Berkovich, A. Shenkman, and G. Golan, "Diode-capacitor voltage multipliers combined with boost-converters: Topologies and characteristics," *IET Power Electron.*, vol. 5, no. 6, pp. 873–884, 2012.
[19] M. Evzelman and S. Ben-Yaakov, "Simulation of hybrid converters by average models," *IEEE Trans. Ind. Appl.*, vol. 50, no. 2, pp. 1106–1113, Mar./Apr. 2014.
[20] M. Evzelman and S. Ben-Yaakov, "Average-current-based conduction losses model of switched capacitor converters," *IEEE Trans. Power Electron.*, vol. 28, no. 7, pp. 3341–3352, Jul. 2013.
[21] M. D. Seeman and S. R. Sanders, "Analysis and optimization of switched-capacitor DC–DC converters," *IEEE Trans. Power Electron.*, vol. 23, no. 2, pp. 841–851, Mar. 2008.

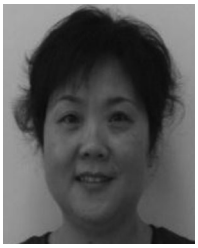

Shiying Hou was born in China, in 1962. She received the B.S., M.S., and Ph.D. degrees from the Department of Electrical Engineering, Chongqing University, Chongqing, China, in 1982, 1999, and 2008, respectively.

She is currently a Professor in the Department of Electrical Engineering, Chongqing University. Her research interests include control theory and its applications, power electronic technology in power systems, and renewable energy grid generation.

Jianfei Chen was born in China, in 1987. He received the B.S. degree from the Department of Electronic Information, Science, and Technology, Chongqing Normal University, Chongqing, China, in 2011. He is currently working toward the M.S. and Ph.D. degrees in the Department of Electrical Engineering, Chongqing University, Chongqing, China.

His research interests include power electronic converters and renewable energy grid generation.

Tao Sun was born in China in 1975. He received the B.S. degree from the Department of Industrial Electrical Automation, Xi'an Petroleum University, Xi'an, China, in 1995, the M.S. degree from the Department of Automatic Control Theory and Application, Sichuan University, Chengdu, China, in 1998, and the Ph.D. degree from the School of Electrical Engineering, Chongqing University, Chongqing, China, in 2005.

From 1998 to 2000, he was with the School of Electrical Engineering, Chongqing University, as a Teaching Assistant and he served there as a Lecturer after 2000. In 2009, he became an Associate Professor in Chongqing University. His research interests include automatic control and power converters.

Xiaohui Bi was born in China, in 1990. He received the B.S. degree from the Department of Electrical Engineering, North China Electric Power University, Beijing, China, in 2013, and is currently working toward the M.S. degree in the Department of Electrical Engineering, Chongqing University, Chongqing, China.

His research interests include renewable energy grid-generation and hybrid energy storage techniques.